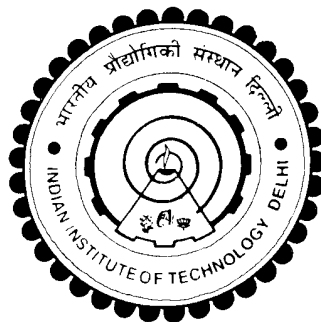


**STUDY OF THE SHIP AIRWAKE AND
HELICOPTER DOWNWASH CHARACTERISTICS
FOR SAFE HELO OPERATIONS**

SHRISH SHUKLA



**DEPARTMENT OF APPLIED MECHANICS
INDIAN INSTITUTE OF TECHNOLOGY DELHI
JUNE 2020**

©Indian Institute of Technology Delhi (IITD), New Delhi, 2020

**STUDY OF THE SHIP AIRWAKE AND
HELICOPTER DOWNWASH CHARACTERISTICS
FOR SAFE HELO OPERATIONS**

by

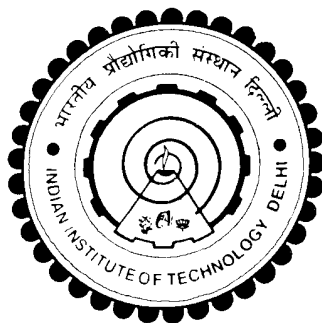
Shrish Shukla

Department of Applied Mechanics

Submitted

In fulfilment of the requirements of the degree of Doctor of Philosophy

to the



INDIAN INSTITUTE OF TECHNOLOGY DELHI

JUNE 2020

I would like to dedicate this thesis to my loving Parents, my sister, Nidhi, and
my brother, Yugraj

CERTIFICATE

This is to certify that the thesis titled " **Study of the Ship Airwake and Helicopter Downwash Characteristics for Safe Helo Operations**" being submitted by **Shrish Shukla**, is report of bonafide research work carried out by him under our supervision. This thesis has been prepared in conformity with the rules and regulations of Indian Institute of Technology, New Delhi, India. We further certify that the thesis has attained a standard required for a Ph. D. degree of the Institute. The research reported and results presented in the thesis have not been submitted, in part or full to any other Institute or University for the award of any degree or diploma.



Dr. S. N. Singh

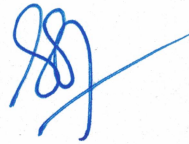
Professor

Dept. of Applied Mechanics,

IIT Delhi,

New Delhi - 110016

INDIA



Dr. S. S. Sinha

Associate Professor

Dept. of Applied Mechanics,

IIT Delhi,

New Delhi - 110016.

INDIA



Dr. R Vijayakumar

Assistant Professor

Dept of Ocean Engineering,

IIT Madras,

Chennai - 600036

INDIA

Date: 22/06/2020

Place: New Delhi

ACKNOWLEDGEMENTS

First of all, my head bows with respect before almighty God who has given me strength, insight and motivation to pursue this work successfully. The cover of this dissertation shows only my name, but some great people have contributed directly or indirectly to this work. I owe my gratitude to all those people who have made this journey possible. It has been a great journey for last three and half years in Indian Institute of Technology Delhi. During this period, I got many opportunities which helped me to explore, learn and develop myself as a competent researcher as well as a good human being. I will cherish forever the time which I have spent at IIT Delhi to purpose this journey.

I would like to take this opportunity to express my sincere gratitude to my research supervisors, Prof. S. N. Singh, Dr. S. S. Sinha and Dr. R. Vijayakumar for their valuable time, constant guidance, and moral support throughout this research work. I have been fortunate to get such intuitive and generous supervisors. You all together have been a tremendous mentor for me. I would like to express my profound regards for encouraging me to grow as a researcher. Your advice on research as well as on my career has been priceless.

I would especially like to express my deep sense of gratitude to Prof. Singh, for extending his support, blessing and act as a parental figure throughout this journey. This journey would not have been possible without your presence. No words can express my gratitude for your valuable advice. Your considerate and compassionate character, your dedication towards the work and most important showing responsibility towards the development of society, inspired me to understand my responsibility towards the nation building, and also helped me to become a better human being. I remain deeply indebted to him for his guidance and faith on me.

I would also like to express my deepest gratitude to Prof. S. S. Sinha for his thought-provoking discussions. All such discussions were very helpful to get good grasp of subject and brought a sense of clarity in my work. His quality of attention to details has helped me to improve my writing and presentation skills immensely. I am big admirer of his teaching style, especially the way he teaches the subject in a very unique and modest way such that the students grasp the concepts comfortably. His quality of dealing the subject with attentive, motivating and exemplary approach ease out the difficult concepts in a very clear and concise way. I have been fortunate to get the opportunity to closely watch his teaching style. I will strive to develop similar skills in near future.

Further, I would also like to express my sincere thanks to Dr. M. Cholemari for extending the support and insights towards to the experimental work. I am also grateful to Dr. S. Nasiruddin, who, as a colleague, as dear friend and as selfless individual, has spent his countless days and assisted and helping me out with learning PIV. The free and frank discussions with him over these years form the very basis and the framework for experiments rigs all that could be achieved. I remain deeply indebted to him for his valuable time.

I would also like to thank Mr. Lakhvinder Singh, who, as a colleague, as a mentor and as a dear friend, has been involved himself into many in-depth discussions during the course of this research work. I have been fortunate to get such exuberant and affectionate co-worker. My gratitude towards him will always remain for the liberty he gave to approach him at any point, despite his busy schedule. I cherish all the time spent with him, especially the leisure time and the meaningful conversations while working together at many sleepless nights.

I would also like to sincerely thank former Experimental Test Pilot of Indian Navy, Cdr KPS Kumar, for taking out valuable time and visiting our premises at multiple occasions to guide

us through the work from the eyes of a pilot. Such crucial and valuable insight gave clarity of thought in attempting solutions for the complex problem.

Further, I would also like to express my gratitude the people who helped me indirectly during this thesis work. I am also thankful to all my lab colleagues; Dr. P. Ranjan, Dr. L. Ragta, Dr. B. Praveen, Dr. B. Babu, Cdr Ishaq Makkar, Lt Cdr Vignesh, Mr. Chandrahas Seth, Mr. Rishav Rajora, Mr. Ramakant Singh, Mr. Nishant Parashar, Mr. Sagar Saroha, Mr. Hammed Hasan, Mr. Sartaj Tanveer, Mr. Harun Ahmad, Mr. Sandeep Yadav and friends for their optimistic views, critical reviews along with valuable suggestions and constructive criticisms.

I would also like to thank my Institution and my departmental research committee faculty members without whom this research work would have been a remote reality. I am very thankful to them. Last, but not the least, I thank my parents for giving me life in the first place, for educating me with all the aspects of life and for unconditional support and encouragement to pursue my interests. I would also like to say thanks to my siblings and all the well-wishers. Finally, I would like to say that this work, which is the significant work of my career, could not have been attempted without the understanding, patience and assistance of my family members. My gratitude is profound.

Shrish Shukla

Date:

Place: New Delhi

ABSTRACT

The operation of helicopters at ships on-board has always been a very complex task owing to the presence of ship air wakes, high velocity gradients, widely varying turbulence length scales as well as the bluff shape ship superstructures. Further, this complexity increases with the addition of helicopter downwash during landing/take off. In addition, these difficulties are more critical for small category frigate class ships. This is mainly due to (i) compactness in shape and size along with fixed design considerations, (ii) the sea-keeping motions encountered in high seas provide a non-stationary oscillating platform, and (iii) the visual cues reduce drastically due to sea spray. Further, the onboard landing deck area is limited (typically twenty percent the entire ship top deck area) due to the vessel stability constraint. In essence, the above-mentioned constraints lead to shipborne helicopter operation being one of the most challenging and difficult tasks in every naval organisation. Hence, an early assessment of the resultant flow environment over the ship helodeck for at early design stage is very crucial to minimise the risk associated with the shipborne helicopter operation.

The study is thus aimed to seek a suitable cost-effective early stage preliminary design tool to evaluate the essential flow features of coupled ship-helo airwake and overcome the complexities associated with shipborne helicopter operations. The study utilises the available experimental and numerical resources to understand the combined ship-helo airwakes characteristics on helodeck contributing to influence the helicopter aerodynamics, and explore solutions for economical early stage approach in order to improve the safe ship-helo operations margin. The ship airwakes and their effect over the flow characteristics of the flight deck region has been analyzed experimentally and computationally. An outstanding problem is to operate a helicopter in the regions of coherent, high-amplitude/less-frequency turbulence flow, which

develop from the sharp edges and additional bluff bodies on the ship superstructure. Therefore, in order to gain insight into the ship airwake characteristics, the experiments have been undertaken on internationally accepted Simplified Frigate Ship (SFS2) along with the helicopter fuselage (ROBIN) at initial stage of investigations. The experimental investigations have been undertaken into two stages. In the first stage, the isolated ship airwake case have been studied experimentally. The combined ship-helo configurations have been extensively investigated with respect to the flight approach path followed on onboard helicopter operations over the helodeck in the second stage of experimental study. Subsequently, the steady flow investigations have been undertaken in order to establish a suitable numerical methodology to reasonably capture the flow characteristics of the experimental studies in the third stage of study.

Subsequently, the fourth stage of study presents a conceptual method to gain insight into the combined ship-helo flow phenomena over a helodeck. One of the prime objectives of this study is to develop an economical design tool employing both experimental as well as computational techniques to simulate the ship-helicopter coupled environment regime at early design stages reasonably well, so as to ease the burden of expensive and risky sea trials. For this purpose, a simplified dynamic interface (SDI) model is proposed to investigate the coupled effects of ship airwake and helicopter downwash. The study reports a parametric analysis to investigate the coupled ship-helo airwake behaviour and its impact on helicopter fuselage over the ship helodeck for different ship speed regimes by the proposed SDI model. The study also reports the influence of 'In Ground Effect' over the helodeck under different downwash conditions.

Further, an attempt has been made to setup preliminary single statistical value-based design criteria to grade the ship-helicopter interface for ensuring minimum standards of safe helo-

operations. The proposed approach is limited to the identification of some dominant resultant coupled ship-helo airwake flow features which influence the helicopter aerodynamics. Results discuss the efficacy of the present approach by highlighting the impact of the coupled flow dynamics in terms of induced fuselage drag, cross-flow characteristics, rotor plane wake and velocity gradients that exist over the helodeck region.’

In the last stage of study, an unsteady flow analysis has been undertaken on isolated ship (SFS2) to establish a suitable unsteady approach for the ship airwake investigations. The overarching aim of this study was to reasonably capture the dominated energy frequency range which affect the onboard helicopter operations. This study provides some insights into the unsteady ship airwake characteristics. Results obtained using three modelling approaches for unsteady ship airwake characteristics namely, Unsteady Reynolds Averaged Navier Stokes (URANS) simulation, Scale Adaptive Simulation (SAS) and Detached Eddy Simulation (DES) discuss the effectiveness of the approaches. The study also attempts to compare mean flow quantities between the unsteady flow approach and steady flow approach

Finally, the proposals for further research have been laid out which are expected to aid in the endeavour towards a complete numerical assessment of the ship-helo interaction problem in future and creation of ship helo operating envelopes (presently created through rigorous First-Of-Class Flying Trials: FOCFT) within the realms of a laboratory.

Keywords: Ship-Helicopter Airwake, Simplified Dynamic Interface (SDI), Helicopter Downwash, Turbulent Flow.

सारांश

जहाजों पर हेलीकाप्टरों का संचालन हमेशा जहाज की हवा की लहरों, उच्च वेग ग्रेडिएंट्स, व्यापक रूप से बदलते हुए एयर टर्बुलेन्स की उपस्थिति और बड़े आकार के जहाज सुपरस्ट्रक्चर के कारण एक बहुत ही जटिल कार्य रहा है। इसके अलावा, लैंडिंग / टेक ऑफ के दौरान हेलीकॉप्टर के डाउनवाश के साथ यह जटिलता काफी बढ़ जाती है। यह कार्य छोटे वर्ग के फ्रिगेट श्रेणी के जहाजों के लिए अत्यधिक जटिल होती है। यह जटिलता मुख्य रूप से (i) जहाज के निश्चित डिजाइन के कारण होता है, (ii) उच्च समुद्र में सामना किए जाने वाले समुद्रीय लहरों की गति के कारण गैर-स्थिर प्लेटफॉर्म प्रदान करती है, और (iii) समुद्रीय लहरों के कारण दृश्य संकेत में भारी गिरावट के कारण होती है। इसके अलावा, जहाज की स्थिरता की कमी के कारण ऑनबोर्ड लैंडिंग डेक क्षेत्र सीमित होता है (आमतौर पर पूरे जहाज के क्षेत्र का सिर्फ बीस प्रतिशत)। संक्षेप में, उपर्युक्त बाधाएं शिपबॉर्न हेलिकॉप्टर ऑपरेशन को जटिल करती हैं जोकी हर नौसेना संगठन में सबसे चुनौतीपूर्ण और कठिन कार्यों में से एक है। इसलिए, शुरुआती डिजाइन चरण के लिए जहाज के हेलोडेक पर परिणामी वायु प्रवाह वातावरण का प्रारंभिक मूल्यांकन शिपबॉर्न हेलिकॉप्टर ऑपरेशन से जुड़े जोखिम को कम करने के लिए बहुत महत्वपूर्ण है।

अतः इस अध्ययन का उद्देश्य युग्मित जहाज-हेलो एयरवेक की आवश्यक प्रवाह विशेषताओं का मूल्यांकन करने और शिपबॉर्न हेलिकॉप्टर संचालन से जुड़ी जटिलताओं को दूर करने के लिए एक उपयुक्त लागत प्रभावी प्रारंभिक प्रारंभिक प्रारंभिक उपकरण की तलाश करना है। हेलिकॉप्टर एयरोडायनामिक्स को प्रभावित करने में योगदान देने वाले हेलोडेक पर संयुक्त जहाज-हीलो एयरवेक विशेषताओं को समझने और सुरक्षित जहाज-हेलो परिचालन मार्जिन में सुधार के लिए किफायती प्रारंभिक चरण दृष्टिकोण के समाधान का पता लगाने के लिए अध्ययन उपलब्ध प्रयोगात्मक और संख्यात्मक संसाधनों का उपयोग करता है। जहाज एयरवेक और उड़ान डेक क्षेत्र की प्रवाह विशेषताओं पर उनके प्रभाव का प्रयोगात्मक और कम्प्यूटेशनल रूप से विश्लेषण किया गया है। एक बकाया समस्या सुसंगत, उच्च-आयाम / कम-

आवृत्ति अशांति प्रवाह के क्षेत्रों में एक हेलीकॉप्टर को संचालित करना है, जो कि जहाज के सुपरस्ट्रक्चर पर तेज किनारों और अतिरिक्त ब्लफ निकायों से विकसित होती है। इसलिए, जहाज एयरवेक विशेषताओं में अंतर्दृष्टि प्राप्त करने के लिए, जांच के प्रारंभिक चरण में हेलीकॉप्टर बॉडी (रोबिन) के साथ अंतरराष्ट्रीय स्तर पर स्वीकृत सरलीकृत फ्रिगेट शिप (एसएफएस 2) पर प्रयोग किए गए हैं। प्रायोगिक जाँच दो चरणों में की गई है। पहले चरण में, पृथक जहाज एयरवेक मामले का प्रयोगात्मक रूप से अध्ययन किया गया है। प्रायोगिक अध्ययन के दूसरे चरण में हेलोडेक पर जहाज पर हेलीकॉप्टर संचालन के बाद उड़ान दृष्टिकोण पथ के संबंध में संयुक्त जहाज-हेलो विन्यास की बड़े पैमाने पर जांच की गई है। इसके बाद, अध्ययन के तीसरे चरण में प्रयोगात्मक अध्ययन के प्रवाह विशेषताओं को यथोचित रूप से पकड़ने के लिए एक उपयुक्त संख्यात्मक पद्धति स्थापित करने के लिए स्थिर प्रवाह जांच की गई है।

इसके बाद, अध्ययन का चौथा चरण एक हेलोडेक पर संयुक्त जहाज-हेलो प्रवाह घटना में अंतर्दृष्टि प्राप्त करने के लिए एक वैचारिक विधि प्रस्तुत करता है। इस अध्ययन के प्रमुख उद्देश्यों में से एक है प्रायोगिक डिजाइन टूल का विकास करना, जिसमें प्रायोगिक तकनीकों के साथ-साथ कम्प्यूटेशनल तकनीकों को नियोजित करना, ताकि जहाज-हेलीकॉप्टर युग्मित पर्यावरण शासन को प्रारंभिक रूप से अच्छी तरह से डिजाइन किया जा सके, ताकि महंगे और जोखिम भरे टेस्टिंग प्रणाली को सरल किया जा सके। इस परीक्षणों के लिए, जहाज एयरवेक और हेलीकॉप्टर डाउनवॉश के युग्मित प्रभावों की जांच करने के लिए एक सरलीकृत गतिशील इंटरफ़ेस (एसडीआई) मॉडल प्रस्तावित है। यह अध्ययन प्रस्तावित एसडीआई मॉडल द्वारा विभिन्न जहाज गति शासनों के लिए जहाज हेलोडेक पर हेलीकॉप्टर पर इसके जहाज-हेलो एयरवेक व्यवहार और इसके प्रभाव की जांच के लिए एक पैरामीट्रिक विश्लेषण की रिपोर्ट करता है। अध्ययन में अलग-अलग डाउनवॉश स्थितियों के तहत हेलोडेक पर 'इन ग्राउंड इफ़ेक्ट' के प्रभाव की भी दर्शाया गया है। इसके साथ-साथ, सुरक्षित हेलो-संचालन के न्यूनतम मानकों को सुनिश्चित करने के लिए जहाज-हेलीकॉप्टर इंटरफ़ेस को ग्रेड करने के लिए प्रारंभिक एकल सांख्यिकीय मूल्य-आधारित डिज़ाइन मानदंड स्थापित करने का प्रयास किया गया है। प्रस्तावित दृष्टिकोण कुछ प्रमुख परिणामी युग्मित जहाज-

हीलो एयरवेक प्रवाह सुविधाओं की पहचान तक सीमित है जो हेलीकॉप्टर वायुगतिकी को प्रभावित करते हैं। परिणाम प्रेरित हेलीकॉप्टर बॉडी ड्रैग, क्रॉस-फ्लो विशेषताओं, रोटरप्लेन वेक और हेलोडेक क्षेत्र में मौजूद वेग गति के संदर्भ में युग्मित प्रवाह की गतिशीलता के प्रभाव को उजागर करके वर्तमान दृष्टिकोण की प्रभावकारिता पर चर्चा करते हैं।

अध्ययन के अंतिम चरण में, जहाज एयरवेक जांच के लिए एक उपयुक्त अस्थिर दृष्टिकोण स्थापित करने के लिए पृथक जहाज (सफस 2) पर एक अस्थिर प्रवाह विश्लेषण किया गया है। इस अध्ययन का व्यापक उद्देश्य वर्चस्व वाली ऊर्जा आवृत्ति रेंज पर केंद्रित है, जो जहाज पर हेलीकॉप्टर संचालन को प्रभावित करते हैं। यह अध्ययन अस्थिर जहाज एयरवेक विशेषताओं में कुछ अंतर्दृष्टि प्रदान करता है। अस्थिर जहाज एयरवेक विशेषताओं के लिए तीन मॉडलिंग दृष्टिकोणों का उपयोग करके प्राप्त किए गए परिणाम, अनस्टेडी रेनॉल्ड्स एवरेज्ड नावियर स्टोक्स (URANS) सिमुलेशन, स्केल एडेप्टिव सिमुलेशन (SAS) और पृथकएडी सिमुलेशन (DES) ने दृष्टिकोण की प्रभावशीलता पर चर्चा की। अध्ययन भी अस्थिर प्रवाह दृष्टिकोण और स्थिर प्रवाह दृष्टिकोण के बीच औसत प्रवाह मात्रा की तुलना करने का प्रयास करता है। अंत में, भावी शोध के प्रस्तावों को निर्धारित किया गया है, जो भविष्य में जहाज-हीलो समस्या के पूर्ण संख्यात्मक मूल्यांकन और जहाज के संचालन के नक्शे के निर्माण की दिशा में सहायता करने की उम्मीद करते हैं।

महत्वपूर्ण शब्दावली: शिप-हेलिकॉप्टर एयरवेक, सरलीकृत डायनामिक इंटरफ़ेस (एसडीआई), हेलीकाप्टर डाउनवॉश, टर्बुलेंट फ्लो।

TABLE OF CONTENTS

CERTIFICATE	I
ACKNOWLEDGEMENTS	III
ABSTRACT	VII
TABLE OF CONTENTS	XI
LIST OF FIGURES.....	XV
LIST OF TABLES.....	XXIII
NOMENCLATURE	XXV
CHAPTER 1. INTRODUCTION	1
1.1. BACKGROUND.....	1
1.2 MOTIVATION.....	4
1.3 OUTLINE OF THE THESIS.....	5
CHAPTER 2. LITERATURE REVIEW	7
2.1 INTRODUCTION.....	7
2.2 FLOW FEATURES OF SHIP AIRWAKE.....	9
2.3 FLOW FEATURES OF HELICOPTER AIRWAKES	11
2.4 COUPLED SHIP-HELO AIRWAKES – THE DYNAMIC INTERFACE.....	13
2.5 EXPERIMENTAL MODELLING.....	14
2.5.1 Mean Flow Characteristics Modelling	14
2.5.2 Unsteady Flow Characteristics Modelling	22
2.6 COMPUTATIONAL MODELLING.....	33
2.6.1 Mean Flow Characteristics Modelling	34
2.6.2 Unsteady Flow Characteristics Modelling	42
2.7 COUPLED SHIP-HELO AIRWAKE MODELLING.....	60
2.8 MARITIME TERMINOLOGY.....	68
2.9 CONCLUSIONS AND GAPS IN KNOWLEDGE FROM LITERATURE REVIEW.....	71

2.10	SCOPE AND OBJECTIVES OF THE PRESENT THESIS	75
CHAPTER 3. EXPERIMENTAL SETUP, INSTRUMENTATION, RESULT AND DISCUSSION		77
3.1	INTRODUCTION.....	77
3.2	EXPERIMENTAL SETUP	78
3.2.1	Wind Tunnel.....	82
3.2.2	Description of the Model Geometries	82
3.3	INSTRUMENTATION	88
3.3.1	Pitot Static Tube.....	88
3.3.2	Manometer	88
3.3.3	Particle Image Velocimetry.....	89
3.4	EXPERIMENTAL PROCEDURE AND PARAMETERS	89
3.4.1	PIV Settings	90
3.4.2	Data Analysis Procedure	92
3.5	SOURCE OF ERROR AND ERROR CALCULATION.....	93
3.5.1	Error Estimate	95
3.6	RANGE OF PARAMETERS AND GEOMETRY CONFIGURATIONS.....	95
3.7	EXPERIMENTAL RESULTS AND DISCUSSIONS	100
3.7.1	Isolated-Ship Airwake Characteristics	101
3.7.2	Combined Ship-Helo Airwake Characteristics	114
3.8	CONCLUDING REMARKS.....	129
CHAPTER 4. MATHEMATICAL FORMULATION, VALIDATION AND RESULTS.....		131
4.1	OVERVIEW OF NUMERICAL METHODS	131
4.2	MATHEMATICAL FORMULATION	135
4.2.1	Reynolds Averaged Navier-Stokes (RANS) Models	136
4.2.2	Scale Adaptive Simulation (SAS) Model.....	140
4.2.3	Detached Eddy Simulation (DES) Model	142
4.3	OVERVIEW OF CFD SOLVER	143
4.3.1	Solver Parameters.....	144

4.3.2	Solver Settings	148
4.4	COMPUTATIONAL METHODOLOGY	152
4.4.1	Modelling Assumptions	153
4.4.2	Geometry Configurations	153
4.4.3	Grid Generation.....	162
4.4.4	Computational Domain and Boundary Conditions	167
4.5	ERROR ESTIMATE.....	170
4.6	VALIDATION OF CFD METHODOLOGY	171
4.6.1	Selection of Turbulence Model.....	171
4.6.2	Grid Independent Study	173
4.6.3	Evaluation of CFD Predictions	178
4.7	FLOW CHARACTERISTICS OF ISOLATED SHIP AND COMBINED SHIP-HELICOPTER	186
4.8	CONCLUDING REMARKS.....	190
 CHAPTER 5. DEVELOPMENT OF A CONCEPTUAL METHOD AND ITS APPLICATION TO ASSESS SHIP-HELICOPTER DYNAMIC INTERFACE.....		191
5.1	INTRODUCTION	191
5.2	BACKGROUND OF SDI MODEL	193
5.2.1	Description of Integrated SDI Assembly	194
5.3	QUANTITY OF INTEREST	195
5.4	COUPLED SHIP-HELO AIRWAKE CHARACTERISTICS.....	199
5.4.1	Fuselage Aerodynamics	200
5.4.2	Downwash Flow Characteristics in Presence of Crossflow	203
5.4.3	Flow Characteristics on Helodeck for Rotor Downwash with Fuselage.....	204
5.4.4	Assessment of Quantity of Interest	212
5.5	STUDY OF THE INFLUENCE OF IN GROUND EFFECT OVER HELODECK	215
5.5.1	Fuselage Aerodynamics	216
5.5.2	Downwash Characteristics	220
5.5.3	Coupled Flow Characteristics	224

5.5.4 Assessment of Quantity of Interest	229
5.6 CONCLUDING REMARKS.....	232
CHAPTER 6. UNSTEADY ANALYSIS OF SHIP AIRWAKES	235
6.1 INTRODUCTION	235
6.2 UNSTEADY CHARACTERISTICS OF SHIP AIRWAKES	238
6.2.1 Validation Study.....	240
6.2.2 Performance Comparison and Discussion.....	243
6.3 CONCLUDING REMARKS	250
CHAPTER 7. CONCLUDING REMARKS AND SUGGESTIONS FOR FUTURE WORK.....	253
7.1 SUMMARY.....	253
7.2 MAJOR CONCLUSIONS	254
7.3 SUGGESTIONS FOR FUTURE WORK.....	256
REFERENCES	259
LIST OF PUBLISHED/COMMUNICATED PAPERS	273

LIST OF FIGURES

Figure 1-1 Typical shipboard helicopter operation: A U.S Navy SH-60 Seahawk helicopter landing on the Singaporean Formidable class frigate ship	2
Figure 2-1 Flow structure behind a three-dimensional bluff body	10
Figure 2-2 Detailed flow features of the backward facing step flow.....	10
Figure 2-3 Ship airwake flow structure on the helodeck	11
Figure 2-4 Rotor blade flow structure as described by Lifting Line Theory	12
Figure 2-5 Typical helicopter downwash airwakes pattern at OGE and IGE conditions.....	12
Figure 2-6 Typical ship-helo coupled airwake flow characteristics	13
Figure 2-7 Basic features of a typical frigate ship geometry	16
Figure 2-8 Schematic of simplified frigate ship (SFS) geometry; SFS2	16
Figure 2-9 Flow of plume exhaust along ship superstructure revealing the smoke trails transportation [24].....	19
Figure 2-10 Schematic of typical One-way Coupled ship-helo environment elements	61
Figure 2-11 Schematic of typical Two-way Coupled ship-helo environment elements.....	61
Figure 2-12 Schematic of typical SHOL envelope	70
Figure 2-13 Schematic of typical DIPES rating	70
Figure 3-1 Schematic diagram of the wind tunnel.....	80
Figure 3-2 Schematic diagram of the test-section with ship model (SFS2-M), laser and camera arrangement.....	81
Figure 3-3 Actual experimental setup in parts	81
Figure 3-4 Dimensional details of the SFS2-M base model (All Dimensions in cm).....	85
Figure 3-5 1:100 Scale model of helicopter fuselage fabricated for wind tunnel experiments	86
Figure 3-6 Dimensional details of the helicopter model (non-dimensional by fuselage length)	86

Figure 3-7 1:100 scale SFS2 ship model, highlighting the locations for mounting the helicopter fuselage	86
Figure 3-8 The combined Ship-Helo model arrangement for wind tunnel experiments	87
Figure 3-9 Schematic of PIV setup data analysis procedure tree [115].....	93
Figure 3-10 Standard ship-based helicopter landing flight path (from Forrest et al. [45]).....	97
Figure 3-11 Schematic of various reference locations of fuselage placement for experiments	97
Figure 3-12 Location of reference planes across the fuselage body	98
Figure 3-13 Comparison of non-dimensional time-averaged resultant velocity contour plots at different elevations over the helodeck for headwind condition; $U_{\infty} = 6$ m/s.....	102
Figure 3-14 Comparison of non-dimensional time-averaged axial velocity contour plots at different elevations over the helodeck for headwind condition; $U_{\infty} = 6$ m/s.....	103
Figure 3-15 Comparison of time-averaged streamlines plots at different elevations over the helodeck for isolated ship configurations at headwind condition; $U_{\infty} = 6$ m/s.....	108
Figure 3-16 Comparison of time-averaged vorticity contour plots at different elevations over the helodeck for headwind condition; $U_{\infty} = 6$ m/s	109
Figure 3-17 Non-dimensional time-averaged axial velocity contour plot (A) and vorticity contour plot (B) for SFS2 at $Z/hHGR = 1.5$ over the helodeck for headwind condition; $U_{\infty} = 6$ m/s...	110
Figure 3-18 Variation of axial and lateral turbulence intensities for isolated SFS2-M configuration at 50% deck length ($X/l_{HDK} = 0.5$)	111
Figure 3-19 Variation of axial (Left) and lateral (Right) turbulence intensities for isolated SFS2 configuration at 50% deck length ($X/l_{HDK} = 0.5$)	111
Figure 3-20 Variation of turbulence intensity ($T.I$) and velocity vector over the helodeck for isolated SFS2 configuration.....	111
Figure 3-21 Comparison of non-dimensional time-averaged axial velocity contour plots at different elevations over the helodeck	119
Figure 3-22 Comparison of time-averaged streamlines plots at different elevations over the helodeck	120

Figure 3-23 Comparison of non-dimensional time-averaged axial velocity contour plots at different elevations over the helodeck	123
Figure 3-24 Comparison of time-averaged streamlines plots at different elevations over the helodeck	124
Figure 3-25 Comparison of non-dimensional time-averaged axial velocity contour plots at different elevations over the helodeck	127
Figure 3-26 Comparison of time-averaged streamlines plots at different elevations over the helodeck	128
Figure 4-1 Control volume and Its nomenclature	149
Figure 4-2 Detail Comparison of ITA and NITA methods [140].....	151
Figure 4-3 Simplified frigate ship: SFS2	154
Figure 4-4 Simplified modified frigate ship without exhaust funnel: SFS2-M.....	155
Figure 4-5 Similarity of flow characteristic region between vertical jet impingement (Left) and rotor downwash at close proximity of ground (Right) [155].....	156
Figure 4-6 Typical helicopter downwash airwakes pattern at OGE (Left) and IGE (Right) conditions [158]	157
Figure 4-7 Schematic of simplified rotor downwash assembly in a wind tunnel: SRD	159
Figure 4-8 Schematic of simplified helicopter fuselage geometry: ROBIN (Isometric view)	161
Figure 4-9 Schematic of integrated simplified dynamic interface configuration: SDI.....	162
Figure 4-10 A cut-section of tetrahedral grid across the ROBIN geometry in centre plane .	163
Figure 4-11 A cut-section of tetrahedral grid across the SFS2 geometry in centre plane	164
Figure 4-12 Schematic of hexahedral grid across the ROBIN geometry	164
Figure 4-13 Schematic of hexahedral grid across the SFS geometry	165
Figure 4-14 Schematic of hybrid grid across the combined SFS2-ROBIN geometry configuration.....	166
Figure 4-15 Schematic of hybrid grid across the integrated SDI geometry configuration....	166
Figure 4-16 Schematic of computational domain boundary conditions	167

Figure 4-17 Non-Dimensional wall distance variation along the ship and fuselage geometry	168
Figure 4-18 Directions of ship and wind velocities	169
Figure 4-19 Comparison of axial velocity profile between the predicted and experimental results at $X/l_{HDK} = 1$, $\psi = 0^0$	172
Figure 4-20 Comparison of normalized resultant velocity across the ship (SFS2)	174
Figure 4-21 Schematic of simplified helicopter fuselage geometry with eight probe sections	175
Figure 4-22 Comparison of ROBIN fuselage surface pressure at $\alpha = 0^0$, $X/R = 0.50$	176
Figure 4-23 Comparison of SRD normalized downwash velocity with full-scale experiment and JAXA's wall jet model at $XDR = 1$	177
Figure 4-24 Comparison of normalized velocity component across the ship for $\psi = 45^0$ wind	179
Figure 4-25 Comparison of normalized mean axial velocity component across the ship beam,	179
Figure 4-26 Comparison of SRD wall jet model with experiment (NASA) and numerical (JAXA) results	181
Figure 4-27 Comparison of ROBIN fuselage surface pressure	181
Figure 4-28 Comparison of normalised axial velocity predictions with in-house experimental	183
Figure 4-29 Comparison of normalised resultant velocity predictions with experimental data	185
Figure 4-30 Comparison of downwash velocity predictions with smoke visualisation data.	185
Figure 4-31 Variation of streamlines over the helodeck for isolated ship configuration at plane $Y/W_b = 0$ and plane $Z/h_{HGR} = 0.5$	187
Figure 4-32 Variation of streamlines over the helodeck for combined ship-helo configuration (Case 8) at plane $Y/W_b = 0$ and plane $Z/h_{HGR} = 0.7$	188
Figure 4-33 Variation of turbulence intensity over the helodeck for combined ship-helo configuration (Case 8) at plane $Y/W_b = 0$ and plane $X/h_{HGR} = 0.7$	189

Figure 5-1 Schematic of integrated SDI assembly: SFS2-M, ROBIN, and SRD.....	195
Figure 5-2 Comparison of fuselage drag coefficient variation at $\psi = 0^\circ$	201
Figure 5-3 Variation of C_d on fuselage at different velocity ratios for $L (D_r/W_b) = 0.42$	201
Figure 5-4 Variation of C_L on fuselage at different velocity ratios for $L (D_r/W_b) = 0.42$	201
Figure 5-5 Variation of C_m on fuselage at different velocity ratios for $L (D_r/W_b) = 0.42$	201
Figure 5-6 Variation of downwash velocity for different velocity ratios along the diameter for a normalized rotor size: $L = 0.42$ at $Y/W_b = 0, Z/h_{HGR} = 1.5$	203
Figure 5-7 Location of various reference planes	205
Figure 5-8 Comparison of non-dimensional resultant velocity contour plots at different velocity ratios, $L = 0.42, \alpha = 0^\circ, \psi = 0^\circ$	206
Figure 5-9 Comparison of recirculation zone by horizontal velocity streamline profile at central plane for $L = 0.42, \alpha = 0^\circ, \psi = 0^\circ$	208
Figure 5-10 Comparison of V_{xy} velocity vector profile at different longitudinal planes for, $L = 0.42, \alpha = 0^\circ, \psi = 0^\circ$	209
Figure 5-11 Comparison of V_{yz} velocity vector profile at different transverse planes for, $L = 0.42, \alpha = 0^\circ, \psi = 0^\circ$	210
Figure 5-12 Variation of mean of the normalised horizontal velocity and normalised mean vertical velocity across the rotor plane (Plane R) for $L = 0.42, \alpha = 0^\circ, \psi = 0^\circ$	214
Figure 5-13 Variation of turbulence intensity across the rotor plane (Plane R) and normalised recirculation length in percentage at height of $Z = 0.09 h_{HGR}$ for $L = 0.42, \alpha = 0^\circ, \psi = 0^\circ$...	214
Figure 5-14 Comparison of induced values of C_d, C_L and C_m of fuselage at different velocity ratio's for constant ship velocity.....	218
Figure 5-15 Comparison of induced values of C_d, C_L and C_m of fuselage at different velocity ratio's for constant downwash velocity	219
Figure 5-16 Downwash flow trajectory at IGE condition for $L = 0.42$ at $\alpha = 0^\circ, \beta = 0.5, \psi = 0^\circ$	222
Figure 5-17 Downwash flow trajectory at IGE condition for $L = 0.84$ at $\alpha = 0^\circ, \beta = 0.5, \psi = 0^\circ$	222

Figure 5-18 Downwash flow trajectory at IGE condition for $L = 1.26$ at $\alpha = 0^0$, $\beta = 0.5$, $\psi = 0^0$	222
Figure 5-19 Downwash flow trajectory at IGE condition for $L = 0.42$ at $\alpha = 0^0$, $\beta = 1$, $\psi = 0^0$	223
Figure 5-20 Downwash flow trajectory at IGE condition for $L = 0.84$ at $\alpha = 0^0$, $\beta = 1$, $\psi = 0^0$	223
Figure 5-21 Downwash flow trajectory at IGE condition for $L = 1.26$ at $\alpha = 0^0$, $\beta = 1$, $\psi = 0^0$	223
Figure 5-22 Comparison of V_{xy} velocity vector profile at different longitudinal planes for, $L=0.42$, $\alpha = 0^0$, $\psi = 0^0$	225
Figure 5-23 Comparison of V_{xy} velocity vector profile at different transverse planes for, $L=0.84$, $\alpha = 0^0$, $\psi = 0^0$	226
Figure 5-24 Comparison of V_{yz} velocity vector profile at different longitudinal planes for, $L=0.42$, $\alpha = 0^0$, $\psi = 0^0$	227
Figure 5-25 Comparison of V_{yz} velocity vector profile at different transverse planes for, $L=0.84$, $\alpha = 0^0$, $\psi = 0^0$	228
Figure 5-26 Variation of mean of the normalised horizontal velocity across the rotor plane (Plane R) at $\alpha = 0^0$, $\psi = 0^0$	230
Figure 5-27 Variation of normalised recirculation length at height of $Z = 0.09 h_{HGR}$ at $\alpha = 0^0$, $\psi = 0^0$	230
Figure 5-28 Variation of mean of the normalised mean vertical velocity across the rotor plane (Plane R) at $\alpha = 0^0$, $\psi = 0^0$	231
Figure 5-29 Variation of turbulence intensity across the rotor plane (Plane R) at $\alpha = 0^0$, $\psi = 0^0$	231
Figure 6-1 Power spectral density of axial velocity fluctuations in the airwake for three different time-steps	241
Figure 6-2 Comparison between experimental [31] and computational (DES) results of mean velocities at $X/h_{DK} = 0.5$, $Z/h_{HGR} = 1$	242

Figure 6-3 Comparison of non-dimensional axial velocity contour plots over the helodeck for (a) Experiment, (b) DES, (c) SAS, (d) URANS, (e) SRANS at $\psi = 0^\circ$, $Z/h_{HGR} = 0.5$245

Figure 6-4 Comparison of Iso-surface of λ_2 value (indicating location of vortex cores) across ship for headwind condition (Top View).....246

Figure 6-5 Time history of normalized vertical velocity at helodeck; probe point $X/l_{LHD} = 0.5$, $Y/W_b = 0$, $Z/h_{HGR} = 0.5$ 248

Figure 6-6 Power spectral density of vertical velocity fluctuations in the airwake.....249

LIST OF TABLES

Table 2-1 The flow characteristics of tuft motion	19
Table 2-2 Important unclassified international regulations of warship/offshore helicopter deck configuration	30
Table 3-1 Description of various ship geometry reported in literature.....	83
Table 3-2 Sources of error in measurements	95
Table 3-3 Details of geometry configuration and range of parameters	98
Table 3-4 Details of various reference locations for measurements.....	99
Table 4-1 Detail feature-based comparison of DNS, LES and RANS method	134
Table 4-2 Details of grids for isolated ship geometry.....	174
Table 4-3 Details of grids for isolated fuselage geometry	175
Table 4-4 Details of grids for isolated SRD geometry	176
Table 6-1 Details of range of parameters.....	238
Table 6-2 Error and time estimate among numerical approaches.....	246

NOMENCLATURE

X, Y, Z	Longitudinal (streamwise), Transverse (spanwise) and Vertical co-ordinate direction
x/X	Normalized streamwise coordinate
y/Y	Normalized cross flow coordinate
z/Z	Normalized spanwise coordinate
u/U	Normalized streamwise velocity
v/V	Normalized cross flow velocity
w/W	Normalized vertical (spanwise) velocity
CTS	Convective Time Scale, defined as L/U_∞ (average time required for a fluid particle to pass the ship)
t^*	Non-dimensional time (t/CTS), in CTS units
t	Physical time (sec)
Δt	Time-step (sec)
Δt^*	Non-dimensional time step ($\Delta t/CTS$)
V_s	Ship velocity
V_a	Atmospheric wind velocity
l	Reference length of the ship
U_∞	Free-stream velocity
V_{ro}	Rotor downwash velocity
V_r	Relative wind velocity, defined as $(V_s - V_a)$
α	Yaw angle of fuselage
β	Velocity ratio (U_∞/U_0)
Ψ	Wind over deck angle (degree)
l_{HDK}	Length of helodeck (m)
h_{HGR}	Height of helo-hangar

L_s, W_s, H_s	Ship length, width, and height
L_d, W_d, H_d	Domain length, width, and height
r_d	Domain radius
Δ	Grid Scaling factor
Δ_0	Grid spacing in the region of interest
τ_w	Wall shear stress
ν_t	Eddy viscosity
μ_t	Dynamic eddy-viscosity
I	Turbulence intensity
k	Turbulent Kinetic Energy
ε	Turbulent dissipation rate
ω	Specific turbulent dissipation rate
St	Strouhal number
f	Natural shedding frequency (Hz)
y^+	Non-dimensional wall length
k	Turbulent kinetic energy (m^2/s^2)
ρ	Density of air (kg/m^3)
P	Mean pressure
Re	Reynolds Number
μ_t	Eddy viscosity
U_∞	Free-stream crossflow velocity (m/s)
U_0	Downwash velocity (m/s)
V_{id}	Induced Velocity (m/s)
u, v, w	Velocity components in x, y, z direction (m/s)
V	Resultant velocity ($\sqrt{u^2 + v^2 + w^2}$)

V_{ref}	Reference velocity ($\sqrt{U_{\infty}^2 + U_0^2}$)
V_n	Normalized resultant velocity (V/V_{ref})
V_{id}	Induced velocity at rotor plane (m/s)
D_r	Rotor diameter (m)
d_0	SRD diameter (m)
T	Rotor thrust (mg)
m	Gross weight of helicopter
g	Acceleration of gravity (m/s^2)
A	Rotor blade swept area ()
L_s	Length of ship (m)
L_f	Length of helicopter fuselage (m)
W_b	Ship beam (m)
W_f	Fuselage width (m)
H_f	Fuselage height (m)
l_{re}	Flow recirculation length (m)
W	Normalized recirculation length (l_{re}/l_{HDK})
L	Normalized rotor size (D_r/W_b)
R	Fuselage length (m)
y^+	Non-dimensional wall distance
I	Turbulent intensity (%)
k	Turbulent kinetic energy (m^2/s^2)
ω	Specific turbulent dissipation rate (s^{-1})
h_0	Rotor height from ground
l_{srd}	Projection length of SRD

Subscripts

i, j, k	Tensor notation
0	Initial conditions
T	Turbulent quantities
i	Inlet
o	Outlet
max	Maximum
min	Minimum

Abbreviations

ABL	Atmospheric Boundary Layer
CFL	Courant-Friedrichs-Lewy number
DDA	Digital Differential Analyzer
D-DES	Delayed Detached Eddy Simulation
DES	Detached Eddy Simulation
DI	Dynamic Interface
DIPES	Deck Interface Pilot Effort Scale
DNS	Direct Numerical Simulation
ETP	Experimental Test Pilot
FOCFT	First-Of-Class Flying Trials
I-LES	Implicit Large Eddy Simulation
POD	Proper Orthogonal Decomposition
PSD	Power Spectral Density
ROBIN	ROtor Body INteraction Fuselage
ROM	Reduced Order Modelling
SAS	Scale Adaptive Simulation

SFS	Simplified Frigate Ship
SHOL	Ship Helicopter Operating Limit
TNT	Turbulent/Non-Turbulent
TTCP	The Technical Cooperation Program
VTOL	Vertical Take-Off and Landing
X-LES	eXtra-Large Eddy Simulation